QUANTIFYING MECHANICAL PROPERTIES OF MATERIAL EXTRUSION FABRICATED LATTICE STRUCTURES BASED ON SEMI-RIGID JOINT FRAME FORMULATION

SANG-IN PARK
George W. Woodruff School of Mechanical Engineering, Georgia Institute of Technology, Atlanta, GA 30332, USA

DAVID W. ROSEN
George W. Woodruff School of Mechanical Engineering, Georgia Institute of Technology, Atlanta, GA 30332, USA

ABSTRACT: This paper presents a new numerical modeling scheme based on the semi-rigid joint frame element formulation for lattice structures fabricated using material extrusion. The proposed scheme has two main elements. First, a modified semi-rigid joint frame element is formulated in order to model struts in lattice structures. Second, a voxel model is developed by simulating the material deposition process; the resulting model geometry is similar to that of the fabricated part. Using this model, effective structural parameters, such as effective strut and joint size and effective joint stiffness, can be computed. Parametric studies were conducted to examine manufacturing effects on the structural parameters. Estimated mechanical properties utilizing the proposed modeling approach are compared with tensile test results for three types of lattice structures. Results demonstrate good predictive capability of the proposed modeling approach.

INTRODUCTION

Lattice structures are engineering materials that consist of periodically arranged representative unit cells. Due to their tailorable mechanical properties, lattice structures have been applied to various fields such as automobile, aerospace and biomedical applications. However, their geometrical complexity makes it hard or impossible to apply conventional manufacturing processes. Recent advances in additive manufacturing (AM) enable lattice structure fabrication using simplified procedures.

When AM processes are used to fabricate lattice structures, many discrepancies occur between the designed geometry and the details of the fabricated shapes [1, 2]. These discrepancies lead to reduced mechanical properties in some AM processes, and property variations in others. For material extrusion processes, the most notable discrepancies are voids, improper filament bonding, and stair-steps [3-5]. The defects become more significant in producing relatively small design features because they are approximated using thin filaments which have finite volume.

Finite element based numerical schemes have been applied in order to estimate mechanical responses of lattice structures. Integrating geometrical defects due to AM process into modeling procedures increases computational resources since modeling small defects decreases mesh size. To realize large lattice structure models, structural elements such as trusses or beams are used with equivalent structural parameters considering manufacturing effects [6]. However, conventional structural elements are not capable of modeling joint effects which reduce effective element length and augment additional stiffness to lattice structures [6, 7]. Semi-rigid jointed frame elements are widely used for large frame structures such as buildings [8, 9]. This element type allows additional structural parameters for joints.

The goal of this paper is to implement a semi-rigid jointed frame element to order to integrate AM process effects into the numerical modeling procedure for lattice structures. The procedure has two

Proc. of the 2nd Intl. Conf. on Progress in Additive Manufacturing
Edited by Chee Kai Chua, Wai Yee Yeong, Ming Jen Tan, Erjia Liu and Shu Beng Tor

Published by Research Publishing, Singapore
ISSN: 2424-8967

$$K_{Torsion} = \begin{bmatrix} k_t & -k_t \\ -k_t & k_t \end{bmatrix} \quad \frac{1}{k_t} = \frac{1}{k_t^{e_1}} + \frac{1}{k_t^{\tilde{L}}} + \frac{1}{k_t^{e_2}}$$
$$k_t^{e_1} = \frac{GJ_{e_1}}{e_1} \frac{\gamma_t^{e_1}}{\left(1-\gamma_t^{e_1}\right)} \quad k^{\tilde{L}} = \frac{GJ_{\tilde{L}}}{\tilde{L}} \quad k_t^{e_2} = \frac{GJ_{e_2}}{e_2} \frac{\gamma_t^{e_2}}{\left(1-\gamma_t^{e_2}\right)} \quad 0 \le \gamma_t^{e_1}, \gamma_t^{e_2} \le 1 \tag{2}$$

where, $k_t^{e_i}$ and $k_t^{\tilde{L}}$ are the joint torsional stiffness and effective torsion bar region stiffness, respectively. $\gamma_t^{e_1}$ and $\gamma_t^{e_2}$ are fixity factors for the torsional stiffness. For flexural stiffness, the joint region is assumed as a rigid beam with a rotational spring at the end of the region, and the frame region in the middle is considered as a conventional shear deformation beam. Two sets of nodal displacements are assumed. One is a nodal displacement vector, $\mathbf{d}^T = \{v_1 \quad \phi_1 \quad v_2 \quad \phi_2\}$, for the entire semi-rigid jointed frame. The other is an internal nodal displacement, $\tilde{\mathbf{d}}^T = \{\tilde{v}_1 \quad \tilde{\phi}_1 \quad \tilde{v}_2 \quad \tilde{\phi}_2\}$, for the frame region as shown in Figure 1. The angle at rotational spring is defined as $\boldsymbol{\alpha}^T = \{0 \quad \alpha_1 \quad 0 \quad \alpha_2\}$. With small displacement assumptions, the relationship between two sets of displacement vectors is derived as $\tilde{\mathbf{d}} = \mathbf{d} + \mathbf{E}(\mathbf{d} - \boldsymbol{\alpha}) - \boldsymbol{\alpha} = (\mathbf{I} + \mathbf{E})(\mathbf{d} - \boldsymbol{\alpha})$. $\mathbf{E}$ represents eccentricity relation matrix. The force-displacement equation for the frame region derives from the conventional shear deformable beam formulation as follows:

$$\begin{Bmatrix} \tilde{V}_1 \\ \tilde{M}_1 \\ \tilde{V}_2 \\ M_2 \end{Bmatrix} = \frac{EI}{(1+\Lambda)\tilde{L}^3} \begin{bmatrix} 12 & 6\tilde{L} & -12 & 6\tilde{L} \\ 6\tilde{L} & (4+\Lambda)\tilde{L}^2 & -6\tilde{L} & (2-\Lambda)\tilde{L}^2 \\ -12 & -6\tilde{L} & 12 & -6\tilde{L} \\ 6\tilde{L} & (2-\Lambda)\tilde{L}^2 & -6\tilde{L} & (4+\Lambda)\tilde{L}^2 \end{bmatrix} \begin{Bmatrix} \tilde{v}_1 \\ \tilde{\phi}_1 \\ \tilde{v}_2 \\ \phi_2 \end{Bmatrix} = \tilde{\mathbf{K}}_b \tilde{\mathbf{d}}, \quad \Lambda = \frac{12EI}{GAK_s\tilde{L}^2}$$

preprocess steps and the layer stacking process are simulated based on deposition path generation and 3D voxel model generation methods. Figure 2 illustrates steps of the proposed as-fabricated voxel model generation procedure. The voxel model is generated by simulating deposition along tool paths. Each layer consists of three sub layers to describe the shape of filaments.

The structural parameters are determined by numerical tensile and bending tests. Theoretically, the axial displacement of a prismatic truss in tension increases linearly through the axial direction based on solid mechanics. However, the resulting displacement field is not linear due to the augmented joint stiffness. The slope of the displacement field near the joints is less than that in the middle of the strut. Figure 3 shows a numerical model and its axial displacement field. The axial displacement from analysis is fitted using three lines for effective joints region and frame region.

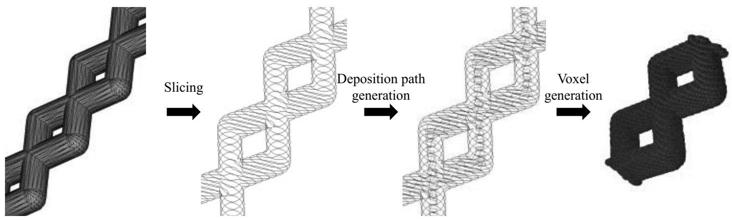

Figure 2 As-fabricated voxel modeling procedure

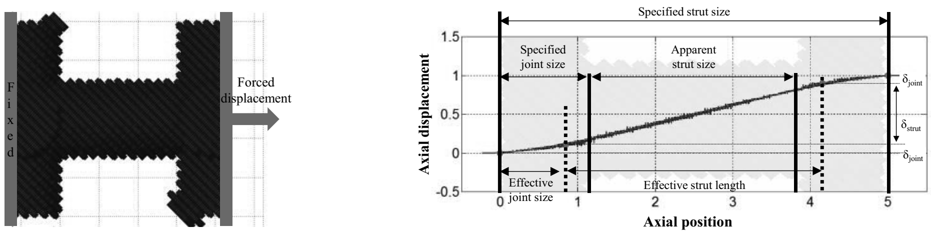

(a) Tensile test **(b) Axial displacement field**

Figure 3 Numerical procedure for determining effective structural parameters

EFFECT OF MATERIAL EXTRUSION ON STRUCTURAL PARAMETERS

Effect of Joint Shape: As joints become larger, the effect of a joint becomes more significant by reducing effective strut length. To examine the effects of the joint shape, four different shapes were selected, as shown in Figure 4. The strut diameters were 2 mm for cubic type unit cells and 1.5 mm for a diamond type unit cell. The mean values of the parameters are listed in Table 1. From the effective strut length and eccentricity of cubic lattice struts, as more struts are overlapped at the joints, the size of the joint increases. The trend of fixity values indicates that a joint becomes stiffer as it becomes larger. In summary joint shape has a large impact on the structural parameters.

Effect of build angle: As-fabricated voxel models were generated with varying build angles with respect to the build direction and the resulting effective structural parameters were calculated. Results are illustrated in Figure 5. Effective strut diameters were reduced up to 10% at a 45 degree building angle. This is because the effect of stair steps increases as the inclined angle approaches 45 degree. The effective joint size and joint stiffness in terms of the eccentricity and fixity decrease as the inclined angle increases.

(a) Cube - 0 overlap **(b) Cube - 3 overlaps** **(c) Cube - 5 overlaps** **(d) Diamond – 4 overlaps**

Figure 4 Joint model

Table 1 Mean value of calculated geometric and structural parameter of 4 types of joints

	Cube – 0 overlap	Cube - 3 overlaps	Cube - 5 overlaps	Diamond – 4 overlaps
Effective strut length / Design length (mm)	3.90 / 5	3.50 / 5	3.38 / 5	1.21 / 2.1651
Effective strut diameter / Design diameter (mm)	1.75 / 2	1.76 / 2	1.76 / 2	1.35 / 1.5
Eccentricity	0.55	0.75	0.81	0.64
Fixity	0.51	0.54	0.58	0.57

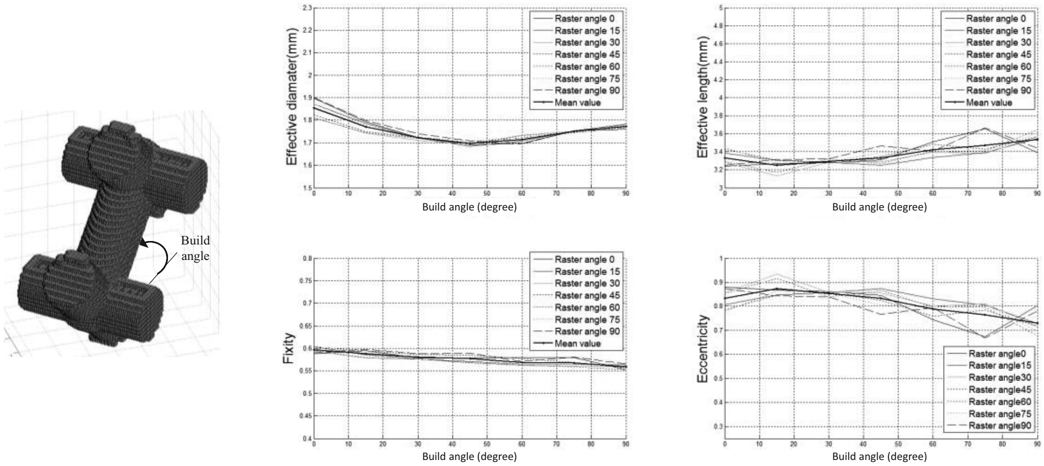

(a) Build angle **(b) Change of effect structural parameters**

Figure 5 Parametric study of varying build angle

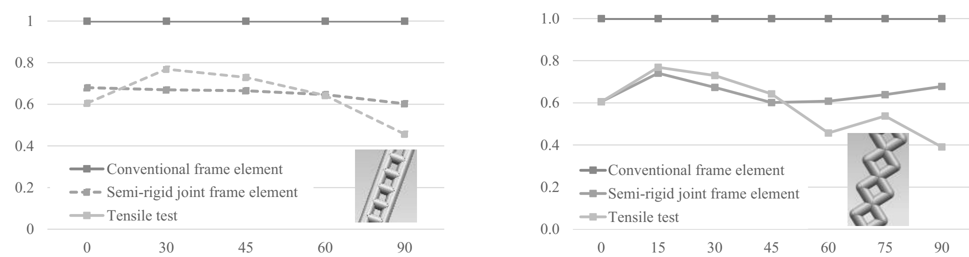

(a) Unit cell 1 **(b) Unit cell 2**

Figure 6 Comparison of elastic modulus

ELASTIC MODULUS ESTIMATION

The proposed as-fabricated modeling procedure was applied to two types of tensile test specimens. The test specimens were fabricated in a Stratasys 1200es machine using ABS P400 material. To study effects of changes in build angle, specimens were built at 0, 15, 30, 45, 60, 75 and 90 degrees. Specimens were modeled using conventional frame elements and the proposed semi-rigid jointed frame elements. The results were compared with tensile test results in Figure 6. The result shows that estimates using conventional elements with designed strut diameters are not capable to integrate manufacturing effects. However, the proposed method can represent effects of geometrical degradation.

CONCLUSION

This research proposed a semi-rigid jointed frame element implementation and effective structural parameter determination procedure with an as-fabricated voxel model. The semi-rigid jointed frame element allows the effects of additive manufacturing to be included in the analysis procedure. Based on the parametric studies, it was found that the joint shape has an impact on the structural parameters and that more overlaps at a joint increase the stiffness of the joint. Results demonstrated that the structural parameters depend on the build angle of the lattice structure. The estimation using the proposed method shows good agreement with the test results. Thus, the proposed method can be applied to the mechanical property estimation procedure for lattice structures from the material extrusion AM process.

ACKNOWLEDGEMENT

The authors gratefully acknowledge support from the National Science Foundation, grant CMMI-1200758. Any opinions, findings, and conclusions or recommendations expressed in this publication are those of the authors and do not necessarily reflect the views of the National Science Foundation.

REFERENCES

1. Campoli, G., Borleffs, M.S., Amin Yavari, S., Wauthle, R., Weinans, H., and Zadpoor, A.A., *Mechanical properties of open-cell metallic biomaterials manufactured using additive manufacturing.* Materials & Design, 2013. **49**: p. 957-965.
2. Ravari, M.R.K., Esfahani, S.N., Andani, M.T., Kadkhodaei, M., Ghaei, A., Karaca, H., and Elahinia, M., *On the effects of geometry, defects, and material asymmetry on the mechanical response of shape memory alloy cellular lattice structures.* Smart Materials and Structures, 2016. **25**(2): p. 025008.
3. Mukesh, K.A., Vikram, R.J., Noshir, A.L., Ahmad, S., Philip, J.W., and Stephen, C.D., *Structural quality of parts processed by fused depositionnull.* Rapid Prototyping Journal, 1996. **2**(4): p. 4-19.
4. Ahn, D., Kweon, J.-H., Kwon, S., Song, J., and Lee, S., *Representation of surface roughness in fused deposition modeling.* J. Materials Processing Technology, 2009. **209**(15–16): p. 5593-5600.
5. Karamooz Ravari, M.R., Kadkhodaei, M., Badrossamay, M., and Rezaei, R., *Numerical investigation on mechanical properties of cellular lattice structures fabricated by fused deposition modeling.* International Journal of Mechanical Sciences, 2014. **88**: p. 154-161.
6. Yang, L., Harrysson, O., Cormier, D., West, H., Gong, H., Stucker, B., *Additive Manufacturing of Metal Cellular Structures: Design and Fabrication.* JOM, 2015. **67**(3): p. 608-615.
7. Kim, H.S. and Al-Hassani, S.T.S., *Effective elastic constants of two-dimensional cellular materials with deep and thick cell walls.* International Journal of Mechanical Sciences, 2003. **45**(12): p. 1999-2016.
8. Monforton, G. and Wu, T.H., *Matrix analysis of semi-rigid connected frames.* Journal of the Structural Division, 1963. **89**(6): p. 13-24.
9. Sekulovic, M. and Salatic, R., *Nonlinear analysis of frames with flexible connections.* Computers & Structures, 2001. **79**(11): p. 1097-1107.